SEPARATIONS

Adsorption Isotherms of Benzoic Acid onto Activated Carbon and Breakthrough Curves in Fixed-Bed Columns

Jia-Ming Chern* and Yi-Wen Chien

Department of Chemical Engineering, Tatung University, 40 Chungshan North Road, 3rd Section, Taipei 10451, Taiwan

The adsorption isotherms of benzoic acid onto granular activated carbon at varying solution temperatures (25−55 °C) and pHs (2−8) from aqueous solution were experimentally determined by batch tests. The Tóth model was found to fit all of the experimental data well. A series of column tests were performed to determine the breakthrough curves with varying bed depths (3−6 cm) and water flow rates (21.6−86.4 cm^3/h). The results show that the half breakthrough time increases proportionally with increasing bed depth but decreases inverse proportionally with increasing velocity. The constant-pattern wave approach using the Freundlich isotherm model fits the experimental breakthrough curves quite successfully. A correlation was proposed to predict the volumetric mass-transfer coefficient in the liquid phase.

Introduction

Benzoic acid (BA) is widely used as a preservative or reaction intermediate and therefore often presents in domestic as well as industrial wastewaters. Because of its harmful effects, wastewaters containing BA must be treated before discharging to receive water bodies. Popular treatment processes include biological degradation,[1−3] chemical oxidation,[4,5] and adsorption.[6−9] Among many adsorbents, granular activated carbon (GAC) is usually used in fixed-bed adsorption processes to remove organic pollutants such as BA.

To properly design and operate fix-bed adsorption processes, the adsorption isotherm and the fix-bed dynamics, that is, the pollutant breakthrough curves, must be known. Various mass-transfer models[10−15] were used to predict the breakthrough curves. To predict the breakthrough curve with a sophisticated mass-transfer model, one needs many parameters that must be determined by independent batch kinetic study or estimated by suitable correlations.[11,14,15] Although a simplified method using one lumped parameter was developed by Wolborska and Pustelnik[12] to predict the breakthrough times of fixed-bed adsorption processes, it can be applied for predicting the breakthrough curve in low concentration ranges with a linear adsorption isotherm only. If we want to predict the whole breakthrough curve, we need a model sophisticated enough to describe the main system features but simple enough to allow for analysis.

A simple yet powerful tool that can be used to predict the breakthrough curves of fixed-bed adsorption processes without tedious calculations is the nonlinear wave propagation theory.[16] In the prediction of the breakthrough curves using the wave propagation theory, an infinite mass-transfer rate must be assumed to fulfill the local equilibrium conditions.[17−19] Unfortunately, this assumption is not always met for fixed beds operated at high flow rates. Therefore, this study adopts the constant-pattern concept of the wave propagation theory along with the constant driving-force model to predict the breakthrough curves of carbon beds for BA removal. The effects of the flow rate and bed depth on the breakthrough curves will be investigated. The adsorption isotherms at varying solution temperatures and pHs will also be measured, and suitable model equations will be tried to fit the experimental data.

Theory

Consider a fixed-bed adsorber packed randomly with adsorbent particles that are fresh or just regenerated, and an aqueous solution containing an organic pollutant is fed to the top of the bed at a constant flow rate. The governing equation for predicting the fixed-bed dynamics is

$$\epsilon \frac{\partial C}{\partial t} + u_0 \epsilon \frac{\partial C}{\partial z} + \rho \frac{\partial q}{\partial t} = 0 \qquad (1)$$

where ρ is the carbon bed density, ρ the void fraction of the bed, u_0 the interstitial velocity of the carrier fluid, t the operating time, and z the distance from the inlet of the mobile phase and C and q are the pollutant concentrations in the mobile and stationary phases, respectively. Equation 1 is basically the unsteady-state mass balance of the adsorbate. The assumptions associated with eq 1 are as follows:

(i) No chemical reactions occur in the column.
(ii) Only mass transfer by convection is significant.
(iii) Radial and axial dispersions are negligible.
(iv) The flow pattern is ideal plug flow.

* To whom correspondence should be addressed. E-mail: jmchern@che.ttu.edu.tw. Tel: 886-2-25925252 ext 3487. Fax: 886-2-25861939.

10.1021/ie010175x CCC: $20.00
Published on Web 07/21/2001

(v) The temperature in the column is uniform and invariant with time.

(vi) The flow rate is constant and invariant with the column position.

The adsorption rate of the pollutant can be described by the linear driving force model in terms of the overall liquid-phase mass-transfer coefficient:[20]

$$\rho \frac{\partial q}{\partial t} = K_L a(C - C^*) \tag{2}$$

where C^* is the mobile-phase concentration in equilibrium with the stationary-phase concentration q, a is the mass-transfer area per unit volume of the bed, and K_L is the overall liquid-phase mass-transfer coefficient. $K_L a$ can be called the volumetric mass-transfer coefficients in the liquid phase.

The initial and boundary conditions associated with eq 1 are

At $t = 0$, $C = 0$ for $0 \le z \le L$

For $t > 0$, at $z = 0$, $C = C_F$

In the language of wave propagation theory,[16] the introduction of the feed generates a self-sharpening wave. Because of the finite mass-transfer rate, the self-sharpening wave will eventually evolve into a constant pattern traveling at a constant velocity, u_C. In the constant-pattern wave, the ratio of the pollutant concentrations in the stationary and mobile phases is constant:[20]

$$\frac{q}{C} = \frac{q_F}{C_F} \tag{3}$$

where C_F is the feed pollutant concentration in the mobile phase and q_F is its associated equilibrium concentration in the stationary phase. Also in the constant-pattern wave, the mobile-phase concentration can be expressed as a unique function of the adjusted time defined as $\tau = t - z/u_C$. The adsorption rate expressed in terms of the adjusted time is

$$\rho \frac{dq}{d\tau} = K_L a(C - C^*) \tag{4}$$

When q is substitiuted with $q_F C/C_F$ into eq 4 and the general adsorption isotherm model of power-law type is used, $q = kC^n$ leads to the following equation that can be used to predict the breakthrough curve:

$$t = t_{1/2} + \frac{\rho k C_F^{\,n-1}}{K_L a}\left[\int_{1/2}^{x} \frac{1}{x - x^{1/n}}\, dx\right] \tag{5}$$

where x is the dimensionless effluent concentration, $x = C/C_F$, and $t_{1/2}$ is the half-time for $x = {}^1/_2$. In eq 5 the parameter $t_{1/2}$ can be directly read from the experimental data and the parameter $K_L a$ can be determined from the tangent slope of the x versus t curve at $x = {}^1/_2$:

$$\left(\frac{dx}{dt}\right)_{x=0.5} = \frac{K_L a}{\rho k C_F^{\,n-1}}(x - x^{1/n}) \tag{6}$$

Experimental Section

BA with purity greater than 99.5% (Fluka Chemical Corp., Switzerland) and distilled deionized water were used to prepare the aqueous solutions for the tests in this study, and the resultant solution pH was called the natural pH. The GAC (Taipei Chemical Corp., Taiwan) was grounded and sieved with U.S. Standard screens to obtain a 24−32 mesh fraction. The sieved GAC was washed with 1 N HCl several times to remove oil and impurity and rinsed repeatedly with deionized water until the rinsed water showed the same UV absorbance intensity as that of the deionized water. Finally, the washed GAC was dried in an oven at 110 °C to constant weight before use. To determine the adsorption isotherms at natural pH and varying solution temperatures, different weights of GAC were added to the glass-stoppered flasks with aqueous solutions having the same BA concentration. Then the flasks were shaken at 150 rpm and the desired temperature in a temperature-controlled shaker (Hotech, model 706) for 4 days to attain equilibrium. The BA concentrations were measured by an UV spectrometer (Milton Roy, model GENE-SYS 5) with the maximum absorbance wavelength at 225 nm and the Lambert−Beer's constant of 13.64. The amounts of BA adsorbed onto the GAC were calculated from the mass balance relation. Various buffer solutions were used to control the solution pH in order to determine the effect of the solution pH on the adsorption isotherm at 25 °C.

The column tests were carried out in a water-jacketed glass column with an inside diameter of 2.77 and a length of 60 cm. The activated carbon with known dried weight was put into the column randomly. Hot deionized water was used to wash the carbon in an upflow fashion in order to remove air bubbles and to rinse the carbon. Then, the bed density and void fraction were determined by the procedures described by Huang[21] before a column test was begun. An aqueous solution with 2.46 mol/m^3 BA concentration at natural pH was continuously fed to the top of the column at a desired flow rate controlled by a metering pump (Watson-Marlow, 302S/RL) until breakthrough happens. In all of the column tests, the effluent samples were intermittently collected by a fraction collector (Isco, Retriever 500) and measured by the UV spectrophotometer. The column temperature was maintained at 25 ± 1 °C, and other test conditions are summarized in Table 1.

Table 1. Experimental Conditions for Column Test Runs

experimental condition	run 1	run 2	run 3	run 4
bed void fraction	0.30	0.30	0.30	0.30
bed density (g/L bed)	277.4	277.4	277.9	277.9
bed depth (cm)	3	3	6	6
flow rate (cm^3/h)	21.6	43.3	43.2	86.4

Results and Discussion

At first, the adsorption isotherms of BA at natural pH and varying solution temperatures were measured and the experimental data were fitted with various isotherm models. The adsorption isotherm models, commonly found in the literature, and their parameters are listed in Table 2. As is indicated by the correlation coefficients, all of the models except the Langmuir model give good fits of the data. Furthermore, the parameters in the Tóth model have clear trends: the maximum adsorption capacity q_m and the dissociation constant m are independent of the solution temperature, while the adsorption equilibrium constant K_1 decreases with increasing temperature. The Gibbs free energy change of the adsorption process is related to the equilibrium

Table 2. Effect of Temperature on the Adsorption Model Parameters for BA at Natural pH

model	equation	parameter	at 25 °C	at 35 °C	at 45 °C	at 55 °C
Langmuir	$q = \frac{KCN}{1 + KC}$	K	18.94	3.47	3.70	3.22
		N	3.22	3.22	2.99	2.67
		R^2	0.94	0.98	0.98	0.95
Freundlich	$q = kC^n$	k	2.92	2.31	2.16	1.87
		n	0.27	0.37	0.33	0.35
		R^2	0.99	0.98	0.96	0.99
Redlich−Peterson	$q = \frac{AC}{B + C^M}$	A	2.98	2.62	2.73	1.90
		B	0.01	0.10	0.19	0.01
		M	0.79	0.77	0.90	0.67
		R^2	1.00	1.00	0.98	0.99
Tóth	$q = \frac{q_m C}{(1/K_1 + C^m)^{1/m}}$	q_m	12.5	12.5	12.5	12.5
		K_1	3.29	2.65	2.55	2.33
		m	0.19	0.19	0.19	0.19
		R^2	0.99	0.97	0.97	0.99

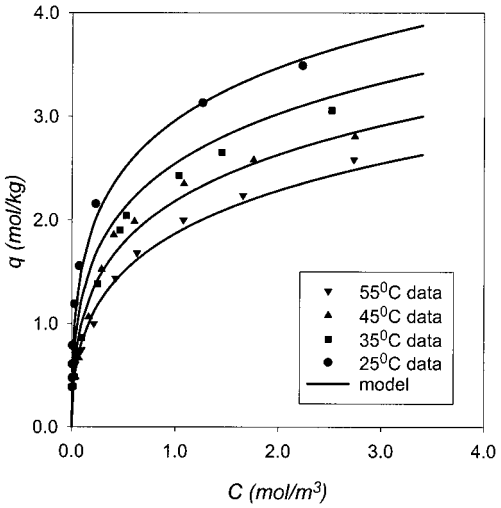

Figure 1. Effect of the solution temperature on the adsorption isotherm of BA at natural pH.

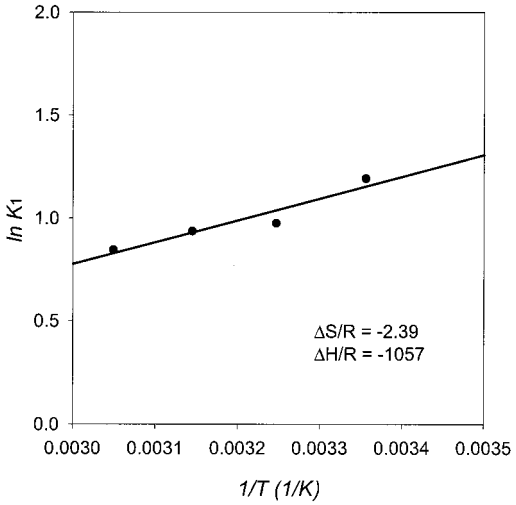

Figure 2. Linear plot of the adsorption equilibrium constant.

constant by the following equation:

$$\Delta G = -RT \ln K_1 \tag{7}$$

According to thermodynamics, the Gibbs free energy change is also related to the entropy change and the heat of adsorption at constant temperature by the following equation:

$$\Delta G = \Delta H - T\Delta S \tag{8}$$

where R is the gas constant, T is the solution temperature, and ΔS and ΔH are the entropy change and heat of adsorption, respectively.

The equilibrium constant K_1 therefore varies with the solution temperature by the following equation:

$$K_1 = \exp\left(\frac{\Delta S}{R} - \frac{\Delta H}{RT}\right) \tag{9}$$

The experimental and Tóth model predicted adsorption isotherms of BA at varying temperatures are shown in Figure 1, and the linear plot of ln K_1 versus $1/T$ is shown in Figure 2. As is shown in Figures 1 and 2, the Tóth model with the equilibrium constant calculated by eq 9 fits the experimental data quite well.

The entropy change and heat of adsorption calculated from the intercept and the slope are −19.9 J/mol·K and −8.8 kJ/mol, respectively. From this low value of the adsorption heat (<40 kJ/mol), we can know that the adsorption of BA onto the GAC is physical adsorption.

The effect of solution pH on the adsorption isotherm was determined at a constant temperature of 25 °C. The adsorption isotherm models listed in Table 2 were also used to fit the experimental data at varying solution pHs. Again, the Tóth model gives a good fit to all of the data, and its model parameters have clear trends: the adsorption equilibrium constant (K_1 = 2.31) and the dissociation constant (m = 0.089) are independent of the solution pH, but the maximum adsorption capacity decreases with increasing solution pH. Figure 3 shows the experimental and predicted adsorption isotherms at varying solution pHs, while Figure 4 shows the maximum adsorption capacity versus solution pH. As is shown in Figures 3 and 4, the Tóth model with the maximum adsorption capacity expressed as a quadratic function of pH can be used to correlate the experimental data successfully. Summers and Roberts[22] reported that the chemical nature of the GAC surface that is influenced by solution pH plays an important role in the adsorption of solutes from aqueous solutions. BA is a weak acid with a pK_a value of 4.2 at 25 °C. At a lower pH, the molecular form is the predominant species, while at a higher pH, the ionized form is the predominant species. Molecular and ionized forms may have different adsorption behaviors onto the GAC surface. A

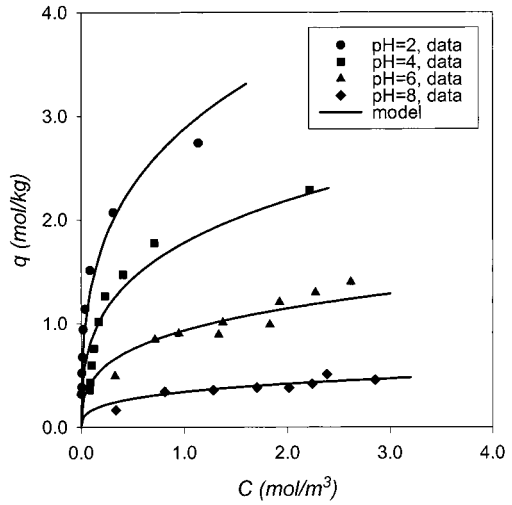

Figure 3. Effect of the solution pH on the adsorption isotherm of BA at 25 °C.

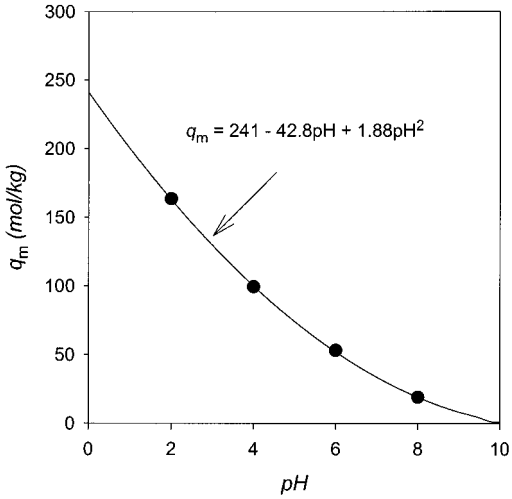

Figure 4. Effect of the solution pH on the maximum adsorption capacity.

more detailed study on the effects of the solution pH on the GAC surface characteristics should be studied in the future.

Although the results of the batch experiments show that the Tóth model is the most reasonable isotherm at varying solution temperatures and pHs, the equilibrium mobile-phase concentration in the Tóth model cannot be expressed as a function of the stationary-phase concentration explicitly. Therefore, the Freundlich model, which fits the isotherm data very well at 25 °C and natural pH ($R^2 = 0.99$), was used in eq 5 to predict the breakthrough curves of the column tests. The effects of the water flow rate on the experimental and predicted breakthrough curves at $L = 3$ and 6 cm are shown in Figures 5 and 6, respectively. The effect of the bed depth on the experimental and predicted breakthrough curves at $Q = 43.2$ cm^3/h is shown in Figure 7. As is shown in Figures 5−7, the constant-pattern wave approach with a constant liquid-phase driving force fits the experimental breakthrough curves well except for a shorter bed depth ($L = 3$ cm) and a slower flow rate ($Q = 21.6$ cm^3/h). In this run, the solid-phase mass-transfer resistance may dominate the overall adsorption rate. A similar result was also discussed by Helfferich and Carr.[23] It is interesting to find that at the same bed depth the half-time, $t_{1/2}$, is inversely proportional to the

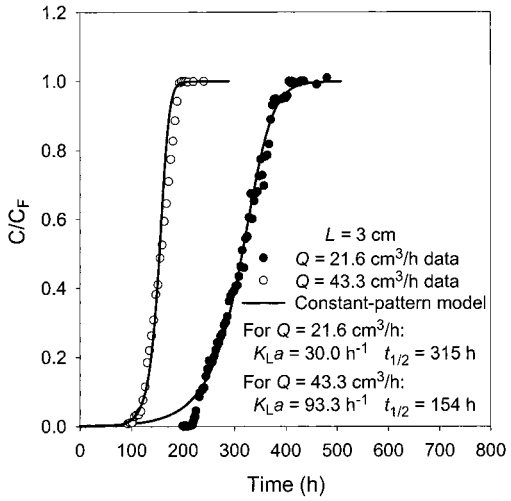

Figure 5. Effect of the feed flow rate on the breakthrough curve at $L = 3$ cm.

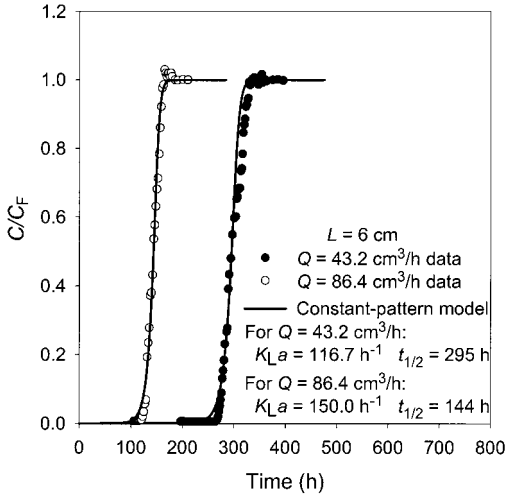

Figure 6. Effect of the feed flow rate on the breakthrough curve at $L = 6$ cm.

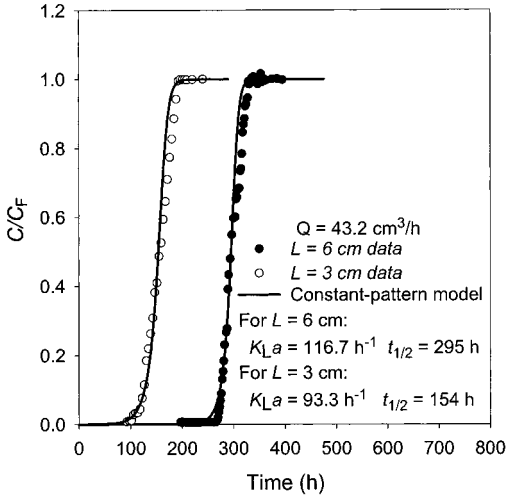

Figure 7. Effect of the bed depth on the breakthrough curve.

water flow rate. At the same water flow rate, the half-time, $t_{1/2}$, is proportional to the bed depth.

There exist many correlations to express the Sherwood number as a function of the Reynolds and Schmidt numbers. A good review of the correlations suggests that the following equation gives the best prediction of the

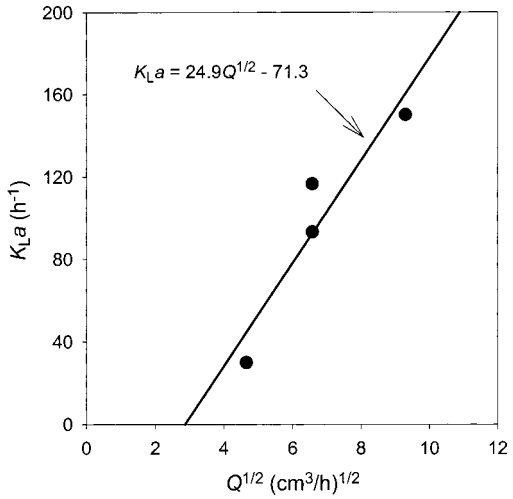

Figure 8. Linear plot of the overall volumetric mass-transfer coefficient.

individual liquid-film mass-transfer coefficient in water treatment situations:[24]

$$Sh = (2 + 0.644Re^{1/2}Sc^{1/3})[1 + 1.5(1 - \epsilon)] \quad (10)$$

where $Sh = d_P k_L/D$, $Re = \rho_L u_0 \epsilon d_P/\mu$, and $Sc = \mu/\rho_L D$.

Using the correlation for k_L and calculating the mass-transfer area per unit bed volume by $a = 6(1 - \epsilon)/d_P$, we found that the volumetric mass-transfer coefficients based on the liquid film only are higher than those determined from the experimental breakthrough curves. For example, $k_L a$, the individual volumetric mass-transfer coefficient calculated from eq 10, is 316 h^{-1} for column test run 4, while $K_L a$, the overall volumetric mass-transfer coefficient determined from the experimental data, is 150 h^{-1}. This suggests that the solid-phase mass-transfer resistance does exist and may have some impact on the breakthrough curve.

According to the results, we propose the following correlation similar to eq 10:

$$K_L a = k_1 + k_2 Q^{1/2} \quad (11)$$

where Q is the volumetric feed flow rate that is proportional to the feed linear velocity u_0. Figure 8 shows the linear plot of $K_L a$ versus $Q^{1/2}$. Equation 11 suggests that the overall liquid-phase volumetric mass-transfer coefficient of a fixed bed is independent of the bed depth but increases with increasing feed flow rate. In the future, more experimental data of wider water flow rate ranges should be collected to further validate eq 11. Furthermore, according to Ruthven,[10] the axial dispersion and mass-transfer resistance play essentially equivalent roles, and the effect of the axial dispersion on the breakthrough curves should also be investigated in the future.

Conclusions

The adsorption isotherms of BA onto GAC at varying solution temperatures and pHs were determined, and the results show that the amounts of BA adsorbed decrease with increasing solution temperature and pH. Among the many adsorption isotherm models, the Tóth model gives the best fit of all of the experimental data and clear trends of parameter variation with the solution temperature and pH. The constant-pattern wave approach has been used to develop explicit equations for the breakthrough curves of fixed-bed adsorption processes with the Freundlich adsorption isotherm. Four column test runs for BA removal were performed, and the results show that the experimental and predicted breakthrough curves are in good agreement. The overall volumetric mass-transfer coefficients in the liquid phase, determined from the experimental data, are less than those predicted by the correlation equation in the literature. Solid-phase mass-transfer resistance has some impact on the overall adsorption rate. A simple equation was proposed to correlate the overall volumetric mass-transfer coefficients in the liquid phase as a function of the feed flow rate satisfactorily.

Acknowledgment

We thank S.-Y. Wang for helping to perform part of the experimental work. The financial support from the National Science Council of Taiwan, Republic of China, is also appreciated.

Nomenclature

a = mass-transfer area per unit volume of the bed [1/m]
C = BA concentration in the mobile phase [mol/m^3]
C_F = BA concentration in the mobile phase [mol/m^3]
C^* = equilibrium BA concentration in the mobile phase [mol/m^3]
d_P = GAC particle diameter [m]
k = Freundlich model parameter [m^{3n}·mol^{1-n}/kg]
k_L = individual liquid-phase mass-transfer coefficient [m/h]
K = Langmuir model parameter [m^3/mol]
K_1 = Tóth model parameter [m^{3m}/mol^m]
K_L = overall liquid-phase mass-transfer coefficient [m/h]
L = bed depth [m]
n = Freundlich model parameter
N = Langmuir model parameter [mol/kg]
q = BA concentration in the stationary phase [mol/kg of dry carbon]
q_F = equilibrium concentration in the stationary phase [mol/kg of dry carbon]
q_m = Tóth model parameter [mol/kg]
Q = volumetric flow rate [m^3/h]
R = gas constant [atm·m^3/mol·K]
t = time [h]
T = solution temperature [K]
$t_{1/2}$ = half-time at $x = {}^1/_2$ [h]
u_0 = interstitial fluid velocity [m/h]
u_C = concentration wave velocity [m/h]
x = dimensionless effluent concentration, $x = C/C_F$
z = distance from the inlet of the mobile phase [m]
ΔH = heat of adsorption [kJ/mol]
ΔS = entropy change of adsorption [kJ/mol·K]
ϵ = void fraction of bed
ρ = carbon bed density [kg/m^3]

Literature Cited

(1) Zachritz, W. H.; Lundie, L. L.; Wang, H. Benzoic acid degradation by small, pilot-scale artificial welands filter (AWF) systems. *Ecol. Eng.* **1996**, *7*, 105−116.

(2) Baumann, U.; Müller, M. T. Determination of anaerobic biodegradability with a simple continuous fixed-bed reactor. *Water Res.* **1997**, *31*, 1513−1517.

(3) Dinsdale, R. M.; Hawkes, F. R.; Hawkes, D. L. Anaerobic digestion of short chain organic acids in an expanded granular sludge bed reactor. *Water Res.* **2000**, *34*, 2433−2438.

(4) Mokrini, A.; Ousse, D.; Esplugas, S. Oxidation of aromatic compounds with UV radiation/ozone/hydrogen peroxide. *Water Sci. Technol.* **1997**, *35*, 95−102.

(5) Chou, S.; Huang, C. Application of a supported iron oxyhydroxide catalyst in oxidation of benzoic acid by hydrogen peroxide. *Chemosphere* **1999**, *38*, 2719−2731.

(6) Yenkie, M. K. N.; Natarajan, G. S. Adsorption equilibrium studies of some aqueous aromatic pollutants on granular activated carbon samples. *Sep. Sci. Technol.* **1991**, *26*, 661−674.

(7) Gusler, G. M.; Browne, T. E.; Cohen, Y. Sorption of organics from aqueous solution onto polymeric resins. *Ind. Eng. Chem. Res.* **1993**, *32*, 2727−2735.

(8) Brasquet, C.; Subrenat, E.; Le Cloirec, P. Selective adsorption on fibrous activated carbon of organics from aqueous solution: correlation between adsorption and molecular structure. *Water Sci. Technol.* **1997**, *35*, 251−259.

(9) Koh, M.; Nakajima, T. Adsorption of aromatic compounds on C_xN-coated activated carbon. *Carbon* **2000**, *38*, 1947−1954.

(10) Ruthven, D. M. *Principles of Adsorption and Adsorption Processes*; Wiley: New York, 1984.

(11) Chatzopoulos, D.; Varma, A. Aqueous-phase adsorption and desorption of toluene in activated carbon fixed beds: experiments and model. *Chem. Eng. Sci.* **1995**, *50*, 127−141.

(12) Wolborska, A.; Pustelnik, P. A Simplified Method for Determination of the Break-Through Time of an Adsorbent Layer. *Water Res.* **1996**, *30*, 2643−2650.

(13) LeVan, M. D.; Carta, G.; Yon, C. M. Adsorption and Ion Exchange. In *Perry's Chemical Engineers' Handbook*, 7th ed.; Perry, R. H., Green, D. W., Maloney, J. O., Eds.; McGraw-Hill: New York, 1997.

(14) Slaney, A. J.; Bhamidimarri, R. Adsorption of pentachlorophenol (PCP) by activated carbon in fixed beds: application of homogeneous surface diffusion model. *Water Sci. Technol.* **1998**, *38*, 227−235.

(15) Wolborska, A. External film control of the fixed bed adsorption. *Chem. Eng. J.* **1999**, *73*, 85−92.

(16) Helfferich, F. G.; Klein, G. *Multicomponent Chromatography*: *Theory of Interference*; Marcel Dekker: New York, 1970.

(17) Chern, J. M.; Huang, S. N. Study of nonlinear wave propagation theory: 1. dye adsorption by activated carbon. *Ind. Eng. Chem. Res.* **1998**, *37*, 253−257.

(18) Chern, J.-M.; Huang, S.-N. Study of Nonlinear Wave Propagation Theory: 2. Interference Phenomena of Single-Component Dye Adsorption Waves. *Sep. Sci. Technol.* **1999**, *34*, 1993−2011.

(19) Chern, J.-M.; Wu, C.-Y. Adsorption of Binary Dye Solution onto Activated Carbon: Isotherm and Breakthrough Curves. *J. CIChE* **1999**, *30*, 507−514.

(20) Sherwood, T. K.; Pigford, R. L.; Wilke, C. R. *Mass Transfer*; McGraw-Hill: New York, 1975; Chapter 10.

(21) Huang, S.-N. Dynamics of Dye Adsorption in Activated Carbon Beds. M.S. Thesis, Tatung University, Taiwan, 1995.

(22) Summers, R. S.; Roberts, P. V. GAC adsorption of humic substances II. Size exclusion and electrostatic interactions. *J. Colloid Interface Sci.* **1988**, *122*, 382−397.

(23) Helfferich, F. G.; Carr, P. W. Nonlinear waves in chromatography I. Waves, shocks, and shapes. *J. Chromatogr.* **1993**, *629*, 97−122.

(24) Roberts, P. V.; Cornal, P.; Summers, R. S. External mass-transfer rate in fixed-bed adsorption. *J. Environ. Eng. Div., ASCE* **1985**, *111*, 891−905.

Received for review February 22, 2001
Revised manuscript received June 4, 2001
Accepted June 8, 2001

IE010175X